Molecular Biology of the Cell
Vol. 12, 3103–3113, October 2001

Zyxin Is not Colocalized with Vasodilator-stimulated Phosphoprotein (VASP) at Lamellipodial Tips and Exhibits Different Dynamics to Vinculin, Paxillin, and VASP in Focal Adhesions[V]

Klemens Rottner,*†‡ Matthias Krause,*‡§ Mario Gimona,† J. Victor Small,† and Jürgen Wehland‡‖

‡Department of Cell Biology, Gesellschaft für Biotechnologische Forschung, D-38124 Braunschweig, Germany; and †Department of Cell Biology, Austrian Academy of Sciences, Institute of Molecular Biology, A-5020 Salzburg, Austria

Submitted February 13, 2001; Revised June 1, 2001; Accepted July 19, 2001
Monitoring Editor: Mary C. Beckerle

Actin polymerization is accompanied by the formation of protein complexes that link extracellular signals to sites of actin assembly such as membrane ruffles and focal adhesions. One candidate recently implicated in these processes is the LIM domain protein zyxin, which can bind both Ena/vasodilator-stimulated phosphoprotein (VASP) proteins and the actin filament cross-linking protein α-actinin. To characterize the localization and dynamics of zyxin in detail, we generated both monoclonal antibodies and a green fluorescent protein (GFP)-fusion construct. The antibodies colocalized with ectopically expressed GFP-VASP at focal adhesions and along stress fibers, but failed to label lamellipodial and filopodial tips, which also recruit Ena/VASP proteins. Likewise, neither microinjected, fluorescently labeled zyxin antibodies nor ectopically expressed GFP-zyxin were recruited to these latter sites in live cells, whereas both probes incorporated into focal adhesions and stress fibers. Comparing the dynamics of zyxin with that of the focal adhesion protein vinculin revealed that both proteins incorporated simultaneously into newly formed adhesions. However, during spontaneous or induced focal adhesion disassembly, zyxin delocalization preceded that of either vinculin or paxillin. Together, these data identify zyxin as an early target for signals leading to adhesion disassembly, but exclude its role in recruiting Ena/VASP proteins to the tips of lamellipodia and filopodia.

INTRODUCTION

Cell migration relies both on the protrusion of motile organelles such as lamellipodia and on the adhesion of cells to the extracellular matrix via specialized sites termed focal adhesions, which link the extracellular substrate to the actin cytoskeleton (reviewed in Horwitz and Parsons, 1999).

Zyxin is found at focal adhesions, cell-cell contacts, and along stress fibers, where it is suggested to play a central role in the regulation of actin dynamics. In addition, several observations indicate a similar role for zyxin at the tips of lamellipodial protrusions. First, the amino terminus of zyxin harbors polyproline-rich stretches, providing binding sites for the SH3 domain of the guanine nucleotide exchange factor for Rho GTPases, Vav (Hobert *et al.*, 1996), and for the EVH1 domain of the Ena/vasodilator-stimulated phosphoprotein (VASP) family proteins VASP and Mena (Gertler *et al.*, 1996; Niebuhr *et al.*, 1997; Drees *et al.*, 2000). Ena/VASP proteins are recruited to the distal edge of lamellipodia in amounts that directly correlate with protrusion rates (Rottner *et al.*, 1999b). Second, ectopical expression of a zyxin-mutant harboring the CAAX membrane-targeting motif causes the induction of actin-rich surface projections (Golsteyn *et al.*, 1997), an effect that is less prominent with a zyxin-CAAX-mutant lacking functional Ena/VASP-binding sites (Drees *et al.*, 2000). Third, microinjection of a zyxin-derived peptide, which blocks the interaction of zyxin with α-actinin, causes the retraction of the cell edge and perturbs cell migration and spreading (Drees *et al.*, 1999). These find-

[V] Online version of this article contains video material for Figure 3, 4, 5, and 7. Online version is available at www.molbiolcell.org.

* K.R. and M.K. contributed equally to this work.
§ Present address: Department of Biology, Massachusetts Institute of Technology, Cambridge, MA 02138-4307.
‖ Corresponding author. E-mail address: jwe@gbf.de.

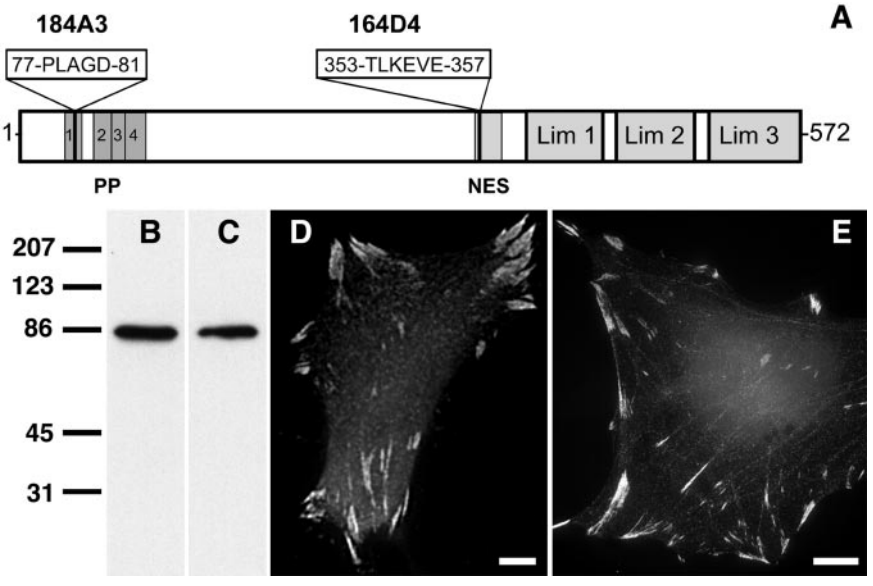

Figure 1. Properties of the generated mAb against zyxin. (A) Schematic representation of the amino acid sequence of zyxin. The four EVH1 binding sites (PP 1–4), nuclear export signal (NES), three LIM domains, and position of the epitopes of both zyxin-specific mAb are indicated. (B and C) Western blot analysis of the zyxin-specific monoclonal antibodies. HeLa cell extracts were separated by SDS-polyacrylamide gel electrophoresis and blotted onto polyvinylidene difluoride membranes. Parallel blots were stained with the antibodies 164D4 (B) and 184A3 (C). Molecular weight markers are indicated on the left. (D and E) Indirect immunofluorescence images of HeLa cells with mAb 164D4 (D) and mAb 184A3 (E) as primary antibodies. Bars, 10 μm.

ings have lead to the proposal that zyxin might serve as a linker, recruiting proteins that contribute to the regulation of actin polymerization at the plasma membrane in a spatially and temporally regulated manner (Goldsteyn *et al.*, 1997; Beckerle, 1998; Jay, 2000; Holt and Koffer, 2001).

Given that VASP is sharply localized to the tips of protruding lamellipodia and filopodia (Rottner *et al.*,1999b), it would be expected from the above-mentioned observations that zyxin shares the same localization. With the use of green fluorescent protein (GFP)-tagged constructs of zyxin as well as a new antibody probe, we found that this was not the case. Our findings, presented here, also provide novel insights into the differential dynamics of zyxin, vinculin, paxillin, and VASP during focal adhesion assembly/disassembly.

MATERIALS AND METHODS

Generation of Antibodies and Western Blotting

Purified zyxin from human platelet extracts was kindly provided by Dr. M. Reinhard (Medizinische Universitätsklinik, Würzburg, Germany) and used to produce monoclonal antibodies in mice as described (Niebuhr *et al.*, 1998). Hybridoma supernatants were screened by immunofluorescence microscopy on HeLa cells and in parallel by Western blot analysis by using total extracts of HeLa cells. By subclass analysis, the monoclonal antibodies, designated 164D4 and 184A3, were identified as IgG1. Spot synthesis was performed according to Frank (1992) with an Abimed ASP 222 automated SPOT robot. Mapping of the epitopes of the monoclonal antibodies was performed as described (Niebuhr *et al.*, 1998).

Total SDS extracts of HeLa cells were separated on 10% SDS gels and electrophoretically transferred to polyvinylidene difluoride membranes. After incubation with the appropriate antibodies, signals were visualized with the use of an enhanced chemiluminescence detection kit (Amersham Pharmacia Biotech AB, Uppsala, Sweden).

Enhanced Green Fluorescent Protein (EGFP)-Constructs

The cDNAs of human zyxin (Macalma *et al.*, 1996) and human paxillin (Salgia *et al.*, 1995) were kindly provided by Dr. D. von der Ahe (Kerckhoff Klinik, Max-Planck Institute, Bad Nauheim, Germany) and Dr. R. Salgia (Harvard Medical School, Boston, MA), respectively. The full-length human zyxin sequence was amplified by polymerase chain reaction with primers containing the restriction sites *Bam*HI/*Eco*RI and cloned into the pEGFP-N1 vector (CLONTECH, Palo Alto, CA). The construct was verified by DNA sequencing. The EGFP-VASP (Carl *et al.*, 1999) and EGFP-paxillin constructs were kindly provided by Dr. U.D. Carl and Marcus Geese, respectively (Gesellschaft für Biotechnologische Forschung, Braunschweig, Germany).

Cells

All reagents were purchased from Invitrogen (Carlsbad, CA) unless stated otherwise. HeLa cells (ATCC CCL-2) and rat embryo fibroblasts (REFs) were maintained in Dulbecco's modified Eagle's medium with 10% fetal calf serum and 1 mM glutamine at 37°C in the presence of 5% CO_2. Mouse melanoma cells B16-F1 (ATCC CRL-6323) were grown as described above except with 10% fetal calf serum from PAA Laboratories (Linz, Austria). Goldfish fin fibroblasts (CAR, ATCC CCL-71) were maintained in basal Eagle's medium with Hanks' balanced salt solution, 1 mM glutamine, 1 mM nonessential amino acids, and 15% fetal bovine serum (Hyclone Laboratories, Logan, UT) at 25°C without CO_2.

Immunolabelings

Indirect immunofluorescence was performed essentially as described previously (Herzog *et al.*, 1994) with minor modifications. Cells were routinely replated onto acid-washed glass coverslips coated with 50 μg/ml fibronectin (Roche Molecular Biochemicals, Mannheim, Germany).

HeLa cells (Figure 1, D and E) were fixed with a mixture of 3% formaldehyde and 0.3% Triton X-100 in cytoskeleton buffer [10 mM 2-(*N*-morpholino)ethanesulfonic acid, 150 mM NaCl, 5 mM EGTA, 5 mM glucose, 5 mM $MgCl_2$, pH 6.1] for 15 min and stained with monoclonal antibodies 164D4 or 184A3 followed by secondary Alexa 546-conjugated goat anti-mouse IgG antibodies (Molecular Probes, Leiden, The Netherlands).

For the double-labeled fluorescence images in Figure 2, B16-F1 cells stably expressing EGFP-VASP were fixed with a mixture of formaldehyde (4%) and 0.1% Triton X-100 in phosphate-buffered

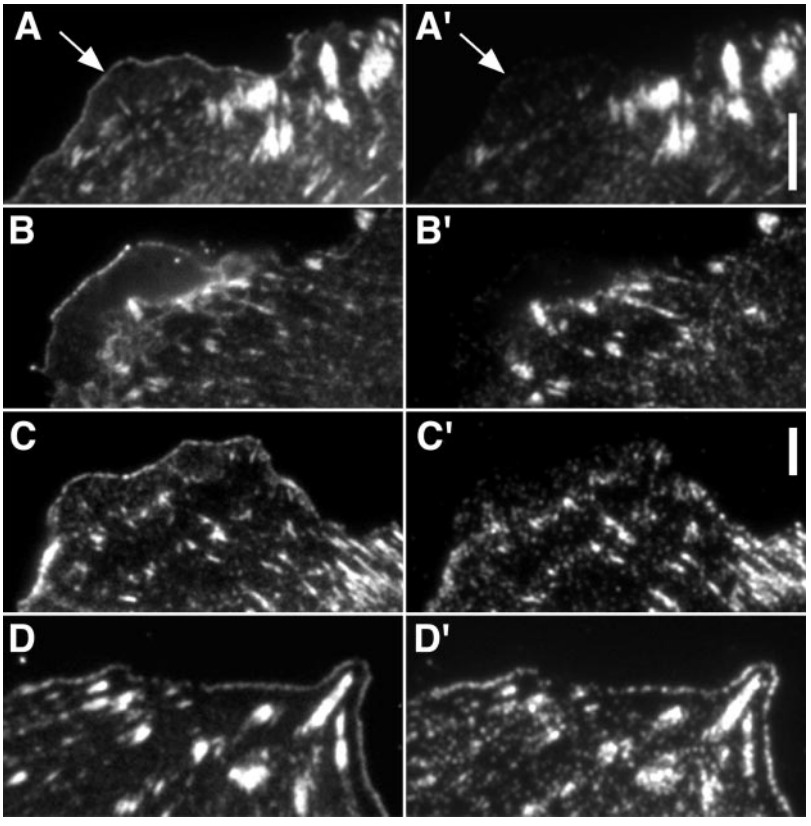

Figure 2. Antibodies against zyxin, vinculin, or paxillin do not counterstain lamellipodial tips containing GFP-VASP. B16-F1 cells transfected with EGFP-VASP (A–D) were plated on fibronectin, fixed, and stained with antibodies to zyxin (164D4) (A′), vinculin (B′), paxillin (C′), and Mena (D′). Note that zyxin, vinculin, and paxillin colocalize with VASP at focal adhesions but not at the tips of lamellipodia (A and A′, arrows), whereas Mena colocalizes with VASP also at these sites. Bars, 5 μm. The bar in C′ is valid for C and C′, and the bar in A′ is valid for all panels except C and C′.

saline, pH 7.0) for 1 min followed by formaldehyde (4%) in phosphate-buffered saline for 20 min. Monoclonal anti-zyxin 164D4, anti-paxillin 349 (Transduction Laboratories, Lexington, KY), anti-vinculin hVIN-1 (Sigma-Aldrich, Taufkirchen, Germany), or monoclonal anti-Mena antibodies (clone 49C2B12; Wehland, unpublished data) were mixed with polyclonal antibodies against GFP (CLONTECH) to enhance the GFP-VASP signal. The secondary reagent was a mixture of Cy3-conjugated goat anti-mouse IgG and fluorescein isothiocyanate-conjugated goat anti-rabbit antibodies (both Jackson Immunoresearch, West Grove, PA). For the α-actinin labelings in Figure 7, cells were fixed on the microscope stage with methanol for 5 min (Mies *et al.*, 1998) and incubated with anti-α-actinin IgM BM.75.2 (Sigma-Aldrich) followed by Cy3-conjugated goat anti-mouse IgM (Jackson Immunoresearch). Pictures of cells fixed and stained on the microscope were taken in cytoskeleton buffer containing 100 mM dithioerythritol (DTE) to avoid photobleaching.

Transfections and Microinjection

B16-F1 cells were transiently transfected with the EGFP-zyxin construct with the use of LipofectAMINE (Invitrogen) as described previously (Ballestrem *et al.*, 1998). At 12–24 h after transfection, B16-F1 cells were replated in Ham's F-12 medium (Invitrogen) containing 10% fetal calf serum onto acid-washed coverslips coated with 25 μg/ml laminin (Sigma-Aldrich) or 50 μg/ml fibronectin.

CAR fibroblasts were transfected with EGFP-VASP or EGFP-paxillin constructs with the use of the Superfect Transfection reagent according to the manufacturer's instructions (QIAGEN, Hilden, Germany). CAR cells were used for microscopy up to 3 d after transient transfections. Stable CAR cell lines (Kaverina *et al.*, 1999) expressing the EGFP-zyxin construct were kindly provided by Dr. I. Kaverina (Austrian Academy of Sciences, Salzburg, Austria). B16-F1, REF, or CAR cells were replated onto 50 μg/ml fibronectin before microinjections.

Injections were performed with sterile Femtotips I (Eppendorf, Hamburg, Germany) with the use of Leitz (Leitz, Austria) or Narishige model M0188NE micromanipulators (Narishige, Tokyo, Japan) with a pressure supply from an Eppendorf microinjector 5242 (Eppendorf). Cells were injected with the back-pressure mode (set to 20–80 hPa) to give a continuous outflow from the needle.

Proteins for Microinjection and Drugs

The fluorescent derivative of turkey gizzard vinculin (5-TAMRA-vinculin) was prepared as described (Rottner *et al.*, 1999a). Recombinant L61Rac was expressed as a glutathione *S*-transferase fusion protein in *Escherichia coli* and purified as described (Ridley and Hall, 1992). Hybridoma supernatant containing anti-zyxin antibodies 164D4 was purified with the use of protein G-Sepharose (Sigma-Aldrich) according to manufacturer's instructions. Purified antibodies were coupled with the use of the Alexa Fluor 488 protein labeling kit (Molecular Probes). After separation of antibodies and excess dye with the use of PD10 columns (Amersham Pharmacia Biotech AB), coupled antibodies were dialyzed into 2 mM Tris, 50 mM KCl, pH 7.0, before microinjection. The purity of proteins was confirmed by Coomassie-stained SDS-polyacrylamide gels and protein concentrations were determined with the use of the Bradford assay (Bio-Rad Laboratories, Munich, Germany). To visualize endogenous zyxin in live cells, Alexa 488-coupled antibodies were microinjected at 1 mg/ml.

To visualize vinculin and zyxin, paxillin, or VASP simultaneously in living cells, 5-TAMRA-vinculin was microinjected at concentrations of 0.5–1 mg/ml into cells expressing EGFP-zyxin, EGFP-paxillin, or EGFP-VASP.

To study the differential dynamics of different adhesion proteins during focal adhesion dissociation in live cells, we developed an assay to transiently but globally mimic the sequence of events taking place during this process. This was achieved by microinjection of CAR cells with mixtures of L61Rac and Y27632 (kindly provided by Yoshitomi Pharmaceutical Industries), an inhibitor of the Rho-associated protein kinase p160ROCK (Uehata *et al.*, 1997). Injection of cells with Y27632 (2.5 mM) alone caused the rapid displacement of EGFP-zyxin, indicative of a down-regulation of the Rho pathway (Ishizaki *et al.*, 1997); however, the cells subsequently retracted their edges, hindering longer term analysis of focal adhesion sites. The addition of L61Rac to the injection mixture further enhanced the dissociation of focal adhesions, presumably due to the antagonistic activities of the Rac and Rho pathways (Hirose *et al.*, 1998; Rottner *et al.*, 1999a). At the same time, the inclusion of Rac facilitated cell spreading and thus allowed analysis of the fate and reformation of focal adhesions throughout the cell. This injection protocol provided a highly reproducible method for inducing rapid disassembly of focal adhesions in live cells. Y27632 was dissolved in microinjection buffer (50 mM Tris pH 7.5, 150 mM NaCl, 5 mM $MgCl_2$, 1 mM DTE) at a concentration of 5 mM and mixed 1:1 with L61Rac (2 mg/ml).

Video Microscopy

B16-F1 and REF cells were observed and microinjected in an open heating chamber (Warner Instruments, Hamden, CT) maintained at 37°C on an inverted microscope (Axiovert 135TV; Zeiss, Jena, Germany) equipped for epifluorescence and phase contrast microscopy. CAR cells were observed and injected at room temperature. For microinjections, 40× objectives (numerical aperture [NA] 0.6 LD Achroplan or NA 1.3 Plan Neofluar; Zeiss) and for video microscopy a 100× objective (NA 1.4 Plan-Apochromat; Zeiss) were used in combination with or without 1.6 optovar intermediate magnification. The microscope was additionally equipped with shutters (Optilas, Puchheim, Germany) in the transmitted and epifluorescence light paths controlled by a homemade interface. A computer-driven filter-wheel (Technical Video, Woods Hole, MA) facilitated separate recordings of video sequences in phase contrast and/or different fluorescence channels. Excitation filters for red and green fluorescence in the filter wheel were used in combination with dichroic beamsplitters and emission filters (Chroma, Brattleboro, VT). Data were acquired with a back-illuminated, cooled charge-coupled device camera (Princeton Research Instruments, Trenton, NJ) driven by IPLab software (Scanalytics, Fairfax, VA), and processed with the use of IPLab, Scion Image 1.62 (Scion, Frederick, MD) and Adobe Photoshop 5.0.2 or 5.5 (Adobe Systems, Mountain View, CA) software.

Quantitation of Focal Adhesion Intensities

Focal adhesions were marked with the use of the segmentation tool in the IPLab software, taking advantage of the fact that adhesions could be identified as structures with intensities above a given threshold level. At least 300 focal adhesions were analyzed for each of the six data groups: zyxin, vinculin, and VASP, each before and 3 min after microinjections with Y27632/Rac. The intensities of focal adhesions were subtracted from the average background intensity in the cytoplasm of each cell (measured at as many points as the number of adhesions). The intensity measurements before treatment were normalized to 100 to pool the data derived from four (3 in the case of VASP) independent cells for each experimental group. The after-treatment data were transformed to percentage of the mean intensities before treatment. Statistical analysis was performed with the use of Microsoft Excel 98 and SigmaStat 2.0, and the graph in Figure 6 was created with Sigma Plot 4.0. The after-treatment data sets were each compared with the before-treatment sets and also with each other with the use of a Mann-Whitney Rank Sum test, from which statistically significant differences could be confirmed ($p < 0001$).

RESULTS

Characterization of Monoclonal Antibodies against Human Zyxin

Two monoclonal antibodies (mAbs) against human zyxin were generated (164D4 and 184A3), and their epitopes were mapped on an array of overlapping synthetic peptides (Frank, 1992; Niebuhr *et al.*, 1998) covering the entire human zyxin sequence (Macalma *et al.*, 1996). This assay enabled the identification of the linear epitopes (Figure 1A; amino acids numbered according to Macalma *et al.*, 1996) recognized by mAb 164D4 (352-TLKEVE-357) and by mAb 184A3 (87-PLAGD-81). The specificity of the monoclonal zyxin antibodies for these epitopes was verified by competitive inhibition with the respective soluble, synthetic peptides). The epitope of the antibody 164D4 maps to the nuclear export signal of zyxin (Nix and Beckerle, 1997), whereas the epitope of 184A3 is localized within the first of the EVH1 domain binding motifs of human zyxin, as defined in Niebuhr *et al.* (1997) (Figure 1A). On Western blots derived from total cell extracts from HeLa cells, both antibodies labeled a single band at ~84 kDa (Figure 1, B and C). In the same cell type, these antibodies predominantly stained focal adhesions (Figure 1, D and E), and in fibroblasts also stress fibers in a periodic manner (Figure 3A). This is in agreement with previous immunofluorescence studies with the use of rabbit antisera increased against a peptide derived from human zyxin (Macalma *et al.*, 1996) and against porcine p83/zyxin (Reinhard *et al.*, 1995). Because 164D4 recognizes a highly conserved zyxin epitope, it labels zyxin in cell lines from several species, including mouse, rat, cow, and pig, whereas mAb 184A3 is more species restricted, both in immunofluorescence microscopy and on Western blots.

Zyxin Is not Recruited to Tips of Protruding Lamellipodia

Because zyxin binds to VASP and Mena (Reinhard *et al.*, 1995; Gertler *et al.*, 1996; Drees *et al.*, 2000) and VASP localizes to the tips of protruding lamellipodia (Rottner *et al.*, 1999b), we next tried to determine whether zyxin and Ena/VASP proteins colocalized at these sites, as proposed previously (Beckerle, 1998).

B16-F1 cells expressing EGFP-VASP were plated on fibronectin and counterstained with our monoclonal anti-zyxin antibody 164D4 (Figure 2, A and A′). Whereas EGFP-VASP localized to the tip of the protruding lamellipodium and to focal adhesions, zyxin only localized to the latter structures (Figure 2, A and A′). A comparison of the localizations of vinculin, paxillin, and Mena in EGFP-VASP-expressing B16-F1 cells is shown in Figure 2, B′–D′. The Mena label matched the distribution of EGFP-VASP entirely (Figure 2, D and D′), indicating that the localization of endogenous proteins at the lamellipodium tip is not affected by fixation. On the other hand, vinculin and paxillin are only found in focal adhesions (Figure 2, B and B′, and C and C′, respectively). In summary, neither zyxin, vinculin, nor paxillin colocalized with VASP and Mena at the tips of lamellipodia.

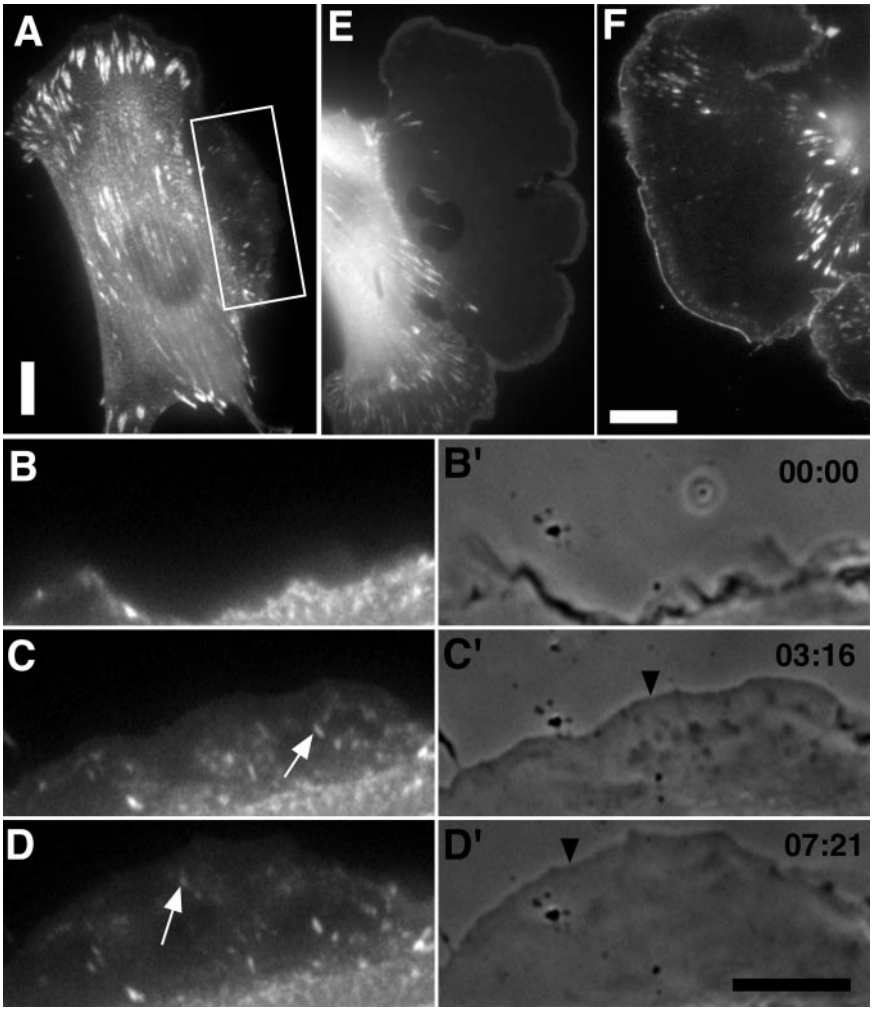

Figure 3. Microinjected mAb 164D4 and ectopically expressed zyxin do not target to lamellipodial tips. (A–D) Representative example of a REF cell microinjected with fluorescently coupled mAb 164D4. (B–D) Video sequence showing an enlargement of the area boxed in the overview in A demonstrates that the fluorescently coupled, microinjected mAb 164D4 does not target to the tip of the protruding lamellipodium (B′ and C′, arrowheads), although it incorporates into newly formed focal adhesions (C and D, arrows; also see video supplement). (E and F) B16-F1 mouse melanoma cells were transiently transfected with EGFP-zyxin or EGFP-VASP to directly compare the dynamics of the respective constructs in these cells moving on laminin. Ectopically expressed EGFP-zyxin (E) is not concentrated at lamellipodial tips, which is sharply contrasted by the dynamics of EGFP-VASP (F) (also see video supplement). Bars, 10 μm (A and F, also valid for E) and 5 μm (D′). *Video Figure 3 B-D*: Dynamics of anti-zyxin mAb 164D4 microinjected into REF cell. Whereas the Alexa 488-coupled mAbs incorporate into stress fibers and focal adhesions, there is no recruitment of antibodies to the tips of the protruding lamellipodium (compare phase contrast). *Video Figure 3 E-F*: B16-F1 cells expressing EGFP-zyxin compared with EGFP-VASP moving on laminin. Both constructs are targeted to focal adhesions. In addition, the motility of these cells induced on this substrate is accompanied by extensive recruitment of EGFP-VASP to the tips of protruding and ruffling lamellipodia. In contrast, EGFP-zyxin is not concentrated at these sites, although there is a slight increase in fluorescence intensity in the entire lamellipodium.

To corroborate the lack of zyxin from lamellipodial tips, we followed the dynamics of this protein in living cells. This was performed in one set of experiments by ectopically expressing EGFP-zyxin, and in another set by microinjecting fluorescently labeled mAb 164D4.

Figure 3A shows a REF cell microinjected with mAb 164D4 coupled to Alexa 488, demonstrating the intense labeling of zyxin in focal adhesions and along stress fibers. Microinjection of this antibody did not affect zyxin dynamics, because adhesion patterns and turnover were not altered for at least 12 h after injection. Figure 3, B–D, shows the dynamics of the fluorescently labeled antibody during extension of the cell periphery (also see video supplement). Although the antibody labels newly formed adhesion sites during this video sequence, there is no concentration of the antibody at the tip of the protruding lamellipodium, as marked by arrowheads in the phase contrast images (Figure 3, C′ and D′).

On laminin, B16-F1 mouse melanoma cells are highly motile and express broad lamellipodia (Ballestrem *et al.*, 1998), providing a useful system to analyze the dynamics of cytoskeletal proteins during cell motility and the protrusion of lamellipodia (Rottner *et al.*, 1999b). Here, we have compared the dynamics of EGFP-zyxin with EGFP-VASP (also see video supplement). Figure 3, E and F, show video frames of B16 cells expressing GFP-tagged zyxin and VASP, respectively. As shown previously, GFP-VASP appears as a sharp line at the edge of protruding lamellipodia (Figure 3F), whereas EGFP-zyxin is incorporated into focal adhesions and stress fibers but not into lamellipodial tips (Figure 3E). The general, diffuse labeling of the lamellipodium in Figure 3E was only marginally more intense than observed with GFP alone.

Comparison of Zyxin and Vinculin Dynamics

To investigate the dynamics of zyxin in more detail, we followed focal adhesion formation in EGFP-zyxin–expressing B16-F1 cells that were previously injected with fluorescently labeled turkey gizzard vinculin (5-TAMRA-vinculin). Comparison of the video sequences showed that both zyxin and vinculin simultaneously incorporated into newly formed adhesion sites at the cell front (Figure 4, A and B, arrows).

However, closer inspection of overall focal adhesion dynamics revealed that zyxin dissociated from dissolving ad-

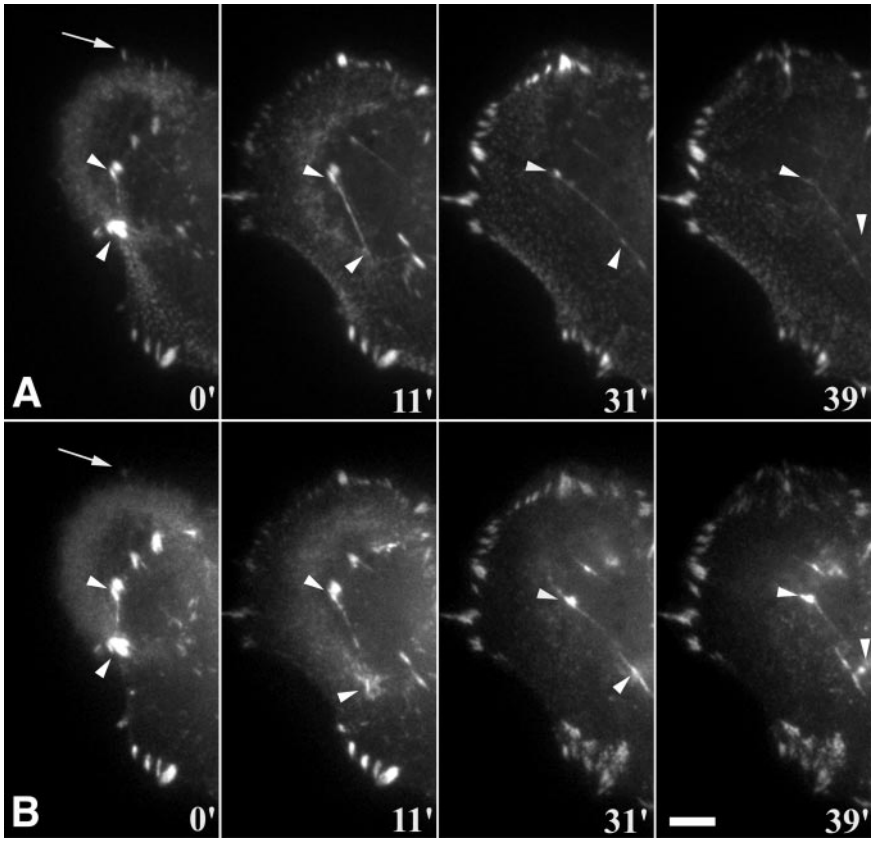

Figure 4. Comparing zyxin with vinculin reveals differential dynamics during adhesion disassembly. B16-F1 cell transiently transfected with EGFP-zyxin and microinjected with rhodamine-labeled vinculin. The video sequence shows the dynamics of zyxin and vinculin in A and B, respectively. Time points of the selected frames are given in minutes. Note that zyxin and vinculin simultaneously incorporate into newly formed adhesion sites (A and B, arrows). In contrast, zyxin clearly dissociates from dissolving focal adhesions earlier than vinculin (A and B, arrowheads). The arrowheads in the top half of the images point toward two adhesion sites, which disappear consecutively in the zyxin panel. By 39′, both sites have disappeared completely, whereas the vinculin picture still shows a prominent adhesion site (compare top arrowheads in A and B, respectively (also see video supplement). The second pair of arrowheads points toward another example showing that as soon as the adhesion site starts sliding (by 11′), zyxin is entirely diminished (also see video supplement). Bar, 10 μm. *Video Figure 4*: Dynamics of EGFP-zyxin and rhodamine-labeled vinculin in B16-F1 cells on fibronectin. Vinculin and zyxin incorporate simultaneously into newly formed adhesions at the cell front (arrows). Conversely, zyxin dissociates from focal adhesions much earlier than vinculin (follow arrowheads). Focal adhesion disassembly is characterized in these cells by the detachment and sliding of vinculin-containing sites (arrowheads), which are devoid of zyxin.

hesions earlier than vinculin, as seen in the video sequence in Figure 4, A and B, arrowheads. To analyze this process in more detail, we used the Rho kinase inhibitor Y27632 (Uehata *et al.*, 1997) to promote focal adhesion disassembly (Rottner *et al.*, 1999a). We established that the injection of goldfish fibroblasts (CAR) with a mixture of Y27632 and constitutively active L61Rac caused the rapid but reversible delocalization of EGFP-zyxin from focal adhesions (compare Figure 5, A and A′; see MATERIALS AND METHODS and video supplement). With the use of this approach we were able to compare the dynamics of different focal adhesion proteins during focal adhesion disassembly.

CAR fibroblasts expressing EGFP-zyxin were first injected with 5-TAMRA-vinculin to record the dynamics of zyxin and vinculin during secondary injections with the Rac/Y27632 mixture. Figure 5, B and C, show the distribution of vinculin and zyxin in the same cell 3 min after the secondary injection, respectively. Before secondary injections, both vinculin and zyxin were strongly incorporated into focal adhesions; (see supplementary video). However, after injections with Rac/Y27632, EGFP-zyxin was rapidly dislocated from focal adhesions (Figure 5C), whereas most of the fluorescent vinculin analog remained in these sites (Figure 5B). To exclude the possibility that the observed effects were due to different labeling methodologies for the two proteins, we performed analogous experiments with cells expressing EGFP-paxillin instead of EGFP-zyxin. In control cells, the EGFP-paxillin construct localized to focal adhesions, as expected from antibody labelings and from previous work (Ludin and Matus, 1998). As shown in Figure 5, 3 min after Rac/Y27632 injection, the distributions of 5-TAMRA-vinculin and EGFP-paxillin were virtually identical (Figure 5, D and E, respectively). EGFP-zyxin–expressing cells that were not injected with 5-TAMRA-vinculin were also injected with Rac/Y27632 and then fixed and stained for paxillin. In line with the findings for vinculin, the focal adhesions had retained paxillin but not zyxin.

Quantitation of the intensities of zyxin and vinculin in focal adhesions of CAR cells immediately before and 3 min after injection of Rac/Y27632 revealed that the treatment reduced the average intensity of zyxin to almost background levels (5%), whereas the average intensity of vinculin fell only 22% below the level before injection (Figure 6). Taken together, these data demonstrate for the first time significant differences between zyxin and vinculin or paxillin with respect to their dynamics during focal adhesion disassembly.

VASP Is Recruited to Focal Adhesions not Only by Zyxin

Zyxin and vinculin harbor binding motifs for the EVH1 domain of Ena/VASP proteins, suggesting that both are required for the recruitment of Ena/VASP proteins to focal adhesions (Gertler *et al.*, 1996). To test this hypothesis, EGFP-VASP–expressing CAR fibroblasts were injected with 5-TAMRA-vinculin followed by secondary injections with

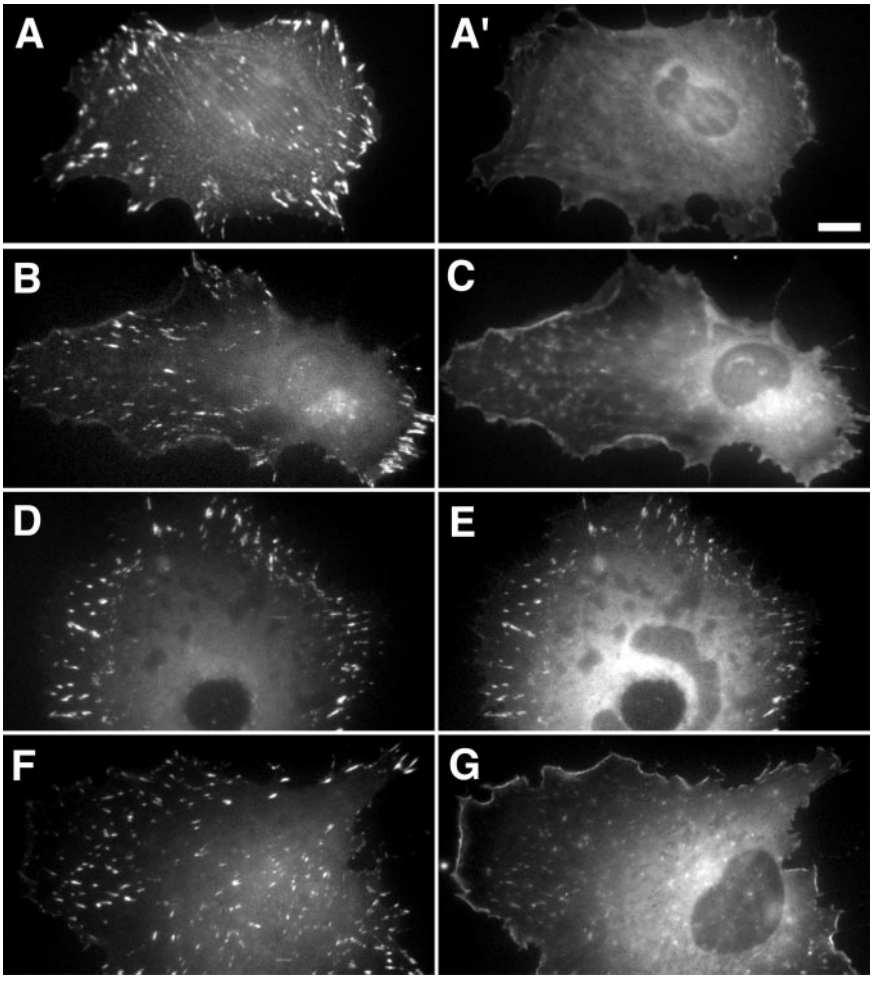

Figure 5. Comparison of various adhesion components during experimentally induced focal adhesion disruption confirms early dissociation of zyxin. Goldfish fibroblasts (CAR) expressing EGFP-zyxin (A) were microinjected with a mixture of constitutively active Rac (L61Rac) and the Rho kinase inhibitor Y27632. A and A′ show the same cell directly before (A) or after microinjection (A′). Before injection, EGFP-zyxin localizes to focal adhesions and stress fibers (A) but is already dislocalized 3 min after microinjection of the L61Rac/Y27632 mixture (A′). (C, E, and G) Examples of CAR fibroblast expressing EGFP-zyxin (C), EGFP-paxillin (E), or EGFP-VASP (G) that have additionally been microinjected first with rhodamine vinculin (B, D, and F) and subsequently with the L61Rac/Y27632 mixture. B, C, and D, E as well as F, G represent image pairs of the same cells 3 min after injection with the secondary mixture, a time point after Rac/Y27632 injection at which zyxin was entirely dislocalized in all experiments performed. In contrast to EGFP-zyxin (C), 5-TAMRA-vinculin (B) still localizes to focal adhesions 3 min after injection, whereas EGFP-paxillin (E) and vinculin (D) behave virtually identically. The intensity of EGFP-VASP (G) in focal adhesions is significantly reduced but not entirely diminished like EGFP-zyxin (C); in contrast, EGFP-VASP is strongly recruited to the tips of the lamellipodia induced by this treatment (G). The cells from all panels except the pair in D, E are provided as supplemental videos. Bar, 10 μm. *Video Figure 5 A-A′*: In an experimental setup to initiate the sequence of events leading to focal adhesion disassembly, EGFP-zyxin–expressing CAR fibroblasts are injected with a mixture of constitutively active Rac and the Rho kinase inhibitor Y27632. Under these conditions, zyxin is rapidly released from focal adhesions. The time point of injection is indicated and can be followed in phase contrast. *Video Figure 5 B-C*: EGFP-zyxin–expressing CAR cells already injected with fluorescent vinculin are injected again with the mixture of L61Rac/Y27632. Whereas zyxin dislocates from focal adhesions very rapidly, the distribution of vinculin remains almost unaffected. This experiment confirms the differential dynamics of vinculin and zyxin during adhesion disassembly observed in untreated cells (as shown in the supplemental video for Figure 4). *Video Figure 5 F-G*: EGFP-VASP–expressing CAR fibroblasts microinjected with rhodamine-labeled vinculin are injected again with the Rac/Y27632 mixture. In contrast with zyxin, this treatment causes a partial loss of VASP from focal adhesions, whereas the distribution of vinculin is again almost unchanged. Note that EGFP-VASP recruitment to the tips of lamellipodia is strongly enhanced by this treatment.

the Rac/Y27632 mixture. This treatment caused a partial dislocation of EGFP-VASP from focal adhesions (Figure 5G; also see supplementary video), whereas the localization of vinculin (Figure 5F; supplementary video) was again almost unaffected. In response to the injection of Rac/Y27632, the behavior of VASP differed from that of both zyxin and vinculin, in that ~47% was dislocated from focal adhesions (Figure 6). These data demonstrate that the recruitment of VASP to focal adhesions is not exclusively mediated by zyxin.

Interestingly, this treatment further illustrated the differential dynamics of zyxin and VASP in lamellipodia. For EGFP-VASP, the partial loss from focal adhesions resulted in a dramatic relocalization to the tips of the induced lamellipodia (Figure 5G), whereas for EGFP-zyxin, no such relocalization was observed, despite active lamellipodial protrusion (Figure 5C).

Displacement of Zyxin from Focal Adhesions Is Accompanied by Depletion of α-Actinin

Because subcellular targeting of zyxin was suggested to be mediated by its interaction with α-actinin (Reinhard *et al.*, 1999), we tested whether experimentally induced dislocation of zyxin by Rac/Y27632 injections was accompanied by dislocation of α-actinin. EGFP-zyxin–expressing CAR fibroblasts were injected with the Rac/Y27632 mixture as before, fixed, and stained with antibodies against α-actinin. Figure 7A shows EGFP-zyxin incorporated into focal adhesions, which is again lost upon injection with Rac/Y27632 (Figure 7A′). At the time of almost complete dislocation of zyxin, the levels of α-actinin, both in focal adhesions and stress fibers, were markedly reduced, compared with noninjected control cells (compare Figure 7, A″ and B). We conclude that the initiation of focal adhesion

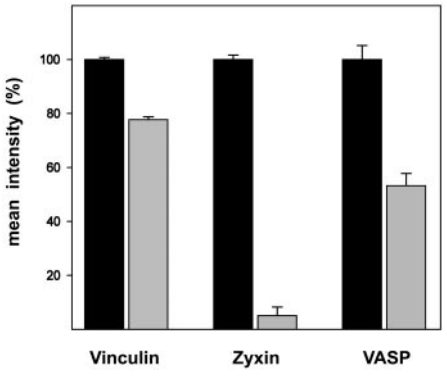

Figure 6. Quantitation of the dislocation of different focal adhesion components in response to injections of Y27632/Rac. Average intensities of focal adhesions were analyzed immediately before (■) and 3 min after microinjection of Y27632/L61Rac (▨) for the different focal adhesions components indicated. Each bar corresponds to the arithmetic mean with SEM.

disassembly coincides with the early displacement of both zyxin and α-actinin.

DISCUSSION

Focal adhesions and lamellipodial tips of fibroblasts are the two sites at which microinjected, fluorescently labeled actin is first incorporated, marking them as centers of actin polymerization (reviewed in Small *et al.*, 1998). Here, the functional similarity stops. Focal adhesions anchor actin filament bundles via transmembrane linkages to the extracellular matrix, whereas lamellipodia are protrusive structures whose tips are highly mobile. We can thus expect that the molecular makeup of the two sites of actin filament generation are correspondingly different. Indeed, the only cytoskeletal components so far found in both sites are Ena/VASP proteins (Rottner *et al.*, 1999b) and profilin (Geese *et al.*, 2000), supporting a general role of these proteins in the dynamic processes of actin reorganization.

Recently, it has been proposed that zyxin may serve as a molecular scaffold, recruiting proteins capable of promoting site-specific actin assembly in lamellipodia (Beckerle, 1998; Drees *et al.*, 1999, 2000). This conclusion is based on immunofluorescence localization studies (Reinhard *et al.*, 1995, Drees *et al.*, 1999) and on data derived from experimentally induced redistribution of zyxin within cells (Golsteyn *et al.*, 1997; Drees *et al.*, 1999, 2000). The retraction of the cell edge after zyxin dislocation was concluded to be caused by the disassembly of molecular complexes regulating actin assembly close to the membrane (Drees *et al.*, 1999). However, this effect may equally well be explained by the disruption of peripheral focal adhesions; thus, myosin II-based contractility is required for the maintenance of focal adhesions (Chrzanowska-Wodnicka and Burridge, 1996) and focal complexes (Rottner *et al.*, 1999a), and the local application of contraction inhibitors was shown to be sufficient to effect the retraction of the cell edge (Kaverina *et al.*, 2000). Interestingly, artificial targeting of zyxin to the membrane by a CAAX motif causes the loss of stress fibers and the induction of F-actin-rich cell "surface projections" (Golsteyn *et al.*, 1997), which are capable of recruiting Ena/VASP proteins (Drees *et al.*, 2000). But this observation does not prove that zyxin is responsible for the recruitment of Ena/VASP proteins to normal actin-mediated cellular protrusions. Rather, the disassembly of stress fibers upon experimentally induced mislocalization of zyxin indicates that zyxin is involved in focal adhesion and stress fiber maintenance.

Our findings clearly demonstrate that in contrast to VASP, zyxin is not present at the protruding tips of lamellipodia, making zyxin an unlikely player in the process of lamellipodial protrusion. We have also noted that the treatment of EGFP-VASP–expressing cells with the Rho kinase inhibitor causes a partial loss of VASP from focal adhesions and a notable incorporation into the tips of the newly protruding lamellipodia. In contrast, the same treatment did not induce a dynamic relocalization of EGFP-zyxin to lamellipodial tips. However, we occasionally observed a weak localization of zyxin throughout the entire width of lamellipodia, for instance, in B16 cells moving on laminin or in fibroblasts

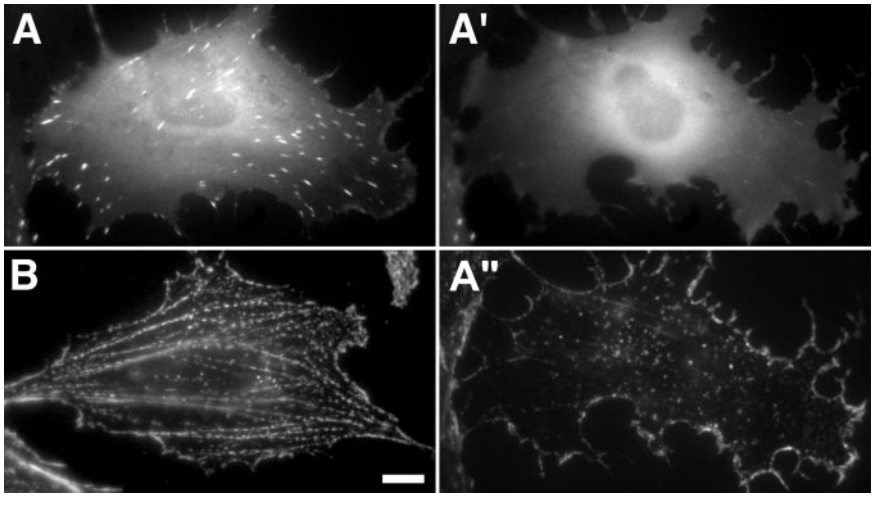

Figure 7. Comparison of zyxin and α-actinin distribution after experimentally induced zyxin displacement. Goldfish fibroblasts (CAR) expressing EGFP-zyxin were microinjected with a mixture of constitutively active Rac (L61Rac) and the Rho kinase inhibitor Y27632. (A and A′) EGFP-zyxin distribution directly before and after microinjection of the mixture, respectively. Cells were fixed right upon virtually complete displacement of EGFP-zyxin. A′ corresponds to the last videoframe before fixation and staining of a representative cell with anti-α-actinin antibodies (A″). Note that at the time of zyxin-displacement, α-actinin was grossly displaced from stress fibers and focal adhesions compared with noninjected neighboring cells (B). Bar, 10 μm.

spreading on fibronectin (Rottner, unpublished data). This is consistent with the presence of its interaction partner α-actinin (Crawford *et al.*, 1992) in lamellipodia (Schulze *et al.*, 1989). Interestingly, zyxin can also be detected at low levels along the actin tail of motile *Listeria monocytogenes* as well as around intracellullar nonmotile bacteria (Frischknecht *et al.*, 1999; Krause and Wehland, unpublished results), where α-actinin is also found (Dabiri *et al.*, 1990; Temm-Grove *et al.*, 1994; Sechi *et al.*, 1997). In contrast, Ena/VASP proteins (Chakraborty *et al.*, 1995) and profilin (Geese *et al.*, 2000) are recruited to the surfaces of *Listeria* where actin monomer insertion occurs, in a situation analogous to lamellipodial tips. These observations further support the view that lamellipodia and the tails of intracellular *Listeria* share similarities with respect to their molecular composition and function (Machesky, 1997). The recruitment of Ena/VASP proteins to the bacterial surface is mediated by FPPPP motifs present in ActA, mimicking a mechanism of positioning of Ena/VASP proteins within the cell by cellular analogs such as vinculin, zyxin, or Fyb/SLAP. The latter protein colocalizes with, and links Ena/VASP proteins to, WASP and the Arp2/3 complex at the interface of T cells and antigen-presenting cells (Krause *et al.*, 2000). However, Fyb/SLAP is restricted to the hematopoetic system and both vinculin and zyxin do not localize at the tips of lamellipodia. Moreover, the cytoplasmic expression of ActA fragments harboring the FPPPP motifs does not interfere with recruitment of Ena/VASP proteins to these sites (Bear *et al.*, 2000). Therefore, at least in nonhematopoetic cells, the targeting of Ena/VASP proteins to the tips of dynamic protrusions such as lamellipodia and filopodia is mediated by an FPPPP-independent mechanism, the nature of which is still controversial (Bear *et al.*, 2000; Nakagawa *et al.*, 2001).

The detailed analysis of zyxin dynamics compared with another prominent focal adhesion protein, vinculin, revealed an intriguing difference. Meigs and Wang (1986) were the first to compare the dynamics of two focal adhesion components in the same cell in response to stimulation by the phorbolester (TPA). They showed that α-actinin was removed before vinculin from focal adhesions and that vinculin persisted until substrate dissociation of these sites, as judged by interference reflection microscopy. Here, we confirm and extend these findings with the use of an assay designed to specifically dissociate focal adhesions. By inhibiting the Rho pathway with the Rho kinase inhibitor Y27632 (Uehata *et al.*, 1997), we show that vinculin and VASP display different dissociation dynamics from zyxin. As an actin filament cross-linker, α-actinin contributes to the maintenance of stress fibers and focal adhesions and presumably performs this role synergistically with myosin and other components. Such a role of α-actinin is further supported by the observation that its overexpression results in the formation of more stable attachment sites, whereas a general reduction of α-actinin synthesis is associated with an increase in cell motility (Glück and Ben-Ze'ev, 1994). One possible partner mediating this postulated role of α-actinin may be zyxin. In agreement with this, we could demonstrate that zyxin dissociates much earlier from dissolving focal adhesions than vinculin and that experimentally induced zyxin dislocation coincides with the displacement of α-actinin, confirming the differential dislocation of α-actinin and vinculin from focal adhesions (Meigs and Wang, 1986). Therefore, the maintenance and integrity of focal adhesions may be influenced by both α-actinin and zyxin. Interestingly, VASP was more tenaciously bound to adhesion sites than zyxin, indicating that VASP recruitment to adhesion sites is not solely dependent on zyxin. Vinculin is one likely candidate responsible for this residual VASP recruitment, because it harbors an FPPPP motif (Brindle *et al.*, 1996; Gertler *et al.*, 1996; Reinhard *et al.*, 1996), but there may be additional focal adhesion proteins involved in this process, such as palladin (Parast and Otey, 2000).

In conclusion, we demonstrate that zyxin does not target Ena/VASP proteins to the tips of lamellipodia. Furthermore, the experimental strategy of simultaneously visualizing the dynamics of two different cytoskeletal proteins within the same cell enabled us to dissect early molecular events upon disintegration of focal adhesions. Our results suggest a role for zyxin in the regulation of focal adhesions and reopen the search for molecules that target Ena/VASP proteins to the tips of lamellipodia and filopodia.

ACKNOWLEDGMENTS

We thank Dr. D. von der Ahe (Kerckhoff Klinik, Max-Planck Institute, Bad Nauheim, Germany) for providing the human zyxin cDNA; Dr. R. Salgia (Harvard Medical School, Boston, MA) for the cDNA of human paxillin; Dr. U.D. Carl and M. Geese for providing EGFP-VASP- and EGFP-paxillin constructs, respectively; and Dr. I. Kaverina (Austrian Academy of Sciences, Salzburg, Austria) for the stable CAR cell line expressing EGFP-zyxin. We thank Yoshitomi Pharmaceutical Industries (Osaka, Japan) for the Rho-kinase inhibitor Y27632, Marlies Konradt and Maria Schmittner for excellent technical assistance, and Dr. A.S. Sechi for helpful discussions. This work was supported in part by the Austrian Science Research Foundation and the Austrian National Bank (to J.V.S.), by the Deutsche Forschungsgemeinschaft (WE 2047/5-1), and the Fonds der Chemischen Industrie (to J.W.). K.R. was supported by European Molecular Biology Organization (fellowship ALTF 164-2000).

REFERENCES

Ballestrem, C., Wehrle-Haller, B., and Imhof, B.A. (1998). Actin dynamics in living mammalian cells. J. Cell Sci. *111*, 1649–1658.

Bear, J.E., Loureiro, J.J., Libova, I., Fassler, R., Wehland, J., and Gertler, F.B. (2000). Negative regulation of fibroblast motility by Ena/VASP proteins. Cell *101*, 717–728.

Beckerle, M.C. (1998). Spatial control of actin filament assembly: lessons from *Listeria*. Cell *95*, 741–748.

Brindle, N.P.J., Holt, M.R., Davies, J.E., Price, C.J., and Critchley, D.R. (1996). The focal-adhesion vasodilator-stimulated phosphoprotein (VASP) binds to the proline-rich domain in vinculin. Biochem. J. *318*, 753–757.

Carl, U.D., Pollmann, M., Orr, E., Gertler, F.B., Chakraborty, T., and Wehland, J. (1999). Aromatic and basic residues within the EVH1 domain of VASP specify its interaction with proline-rich ligands. Curr. Biol. *9*, 715–718.

Chakraborty, T., Ebel, F., Domann, E., Niebuhr, K., Gerstel, B., Pistor, S., Temm-Grove, C.J., Jockusch, B.M., Reinhard, M., Walter, U., et al. (1995) A focal adhesion factor directly linking intracellularly motile *Listeria monocytogenes* and *Listeria ivanovii* to the actin-based cytoskeleton of mammalian cells. EMBO J. *14*, 1314–1321.

Chrzanowska-Wodnicka, M. and Burridge, K. (1996). Rho-stimulated contractility drives the formation of stress fibers and focal adhesions. J. Cell Biol. *133*, 1403–1415.

Crawford, A.W., Michelsen, J.W., and Beckerle, M.C. (1992). An interaction between zyxin and α-actinin. J. Cell Biol. *116*, 1381–1393.

Dabiri, G.A., Sanger, J.M., Portnoy, D.A., and Southwick, F.S. (1990). *Listeria monocytogenes* moves rapidly through the host-cell cytoplasm by inducing directional actin assembly. Proc. Natl. Acad. Sci. USA *87*, 6068–6072.

Drees, B., Andrews, K.M., and Beckerle, M.C. (1999). Molecular dissection of zyxin function reveals its involvement in cell motility. J. Cell Biol. *147*, 1549–1559.

Drees, B.E., Friederich, E., Fradelizi, J., Louvard, D., Beckerle, M.C., and Golsteyn, R.M. (2000). Characterization of the interaction between zyxin, and members of the Ena/vasodilator-stimulated phosphoprotein family of proteins. J. Biol. Chem. *275*, 22503–22511.

Frank, R. (1992). Spot synthesis: an easy technique for the positionally addressable, parallel chemical synthesis on a membrane support. Tetrahedron *48*, 9217–9232.

Frischknecht, F., Cudmore, S., Moreau, V., Reckmann, I., Rottger, S., and Way, M. (1999). Tyrosine phosphorylation is required for actin-based motility of *Vaccinia* but not *Listeria* or *Shigella*. Curr. Biol. *9*, 89–92.

Geese, M., Schluter, K., Rothkegel, M., Jockusch, B.M., Wehland, J., and Sechi, A.S. (2000). Accumulation of profilin II at the surface of *Listeria* is concomitant with the onset of motility, and correlates with bacterial speed. J. Cell Sci. *113*, 1415–1426.

Gertler, F.B., Niebuhr, K., Reinhard, M., Wehland, J., and Soriano, P. (1996). Mena, a relative of VASP and *Drosophila* Enabled, is implicated in the control of microfilament dynamics. Cell *87*, 227–239.

Glück, U., and Ben-Ze'ev, A. (1994). Modulation of α-actinin levels affects cell motility and confers tumorigenicity on 3T3 cells. J. Cell Sci. *107*, 1773–1782.

Golsteyn, R.M., Beckerle, M.C., Koay, T., and Friedrich, E. (1997). Structural and functional similarities between the human cytoskeletal protein zyxin and the ActA protein of *Listeria monocytogenes*. J. Cell Sci. *110*, 1893–1906.

Herzog, M., Draeger, A., Ehler, E., and Small, J.V. (1994). Immunofluorescence microscopy of the cytoskeleton: double and triple immunoflurescence. In: Cell Biology: A Laboratory Handbook, ed. J.E. Celis, San Diego, CA: Academic Press, 355–360.

Hirose, M., Ishizaki, T., Watanabe, N., Uehata, M., Kranenburg, O., Moolenaar, W.H., Matsumura, F., Maekawa, M., Bito, H., and Narumiya, S. (1998). Molecular dissection of the Rho-associated protein kinase (p160ROCK)-regulated neurite remodeling in neuroblastoma N1E-115 cells. J. Cell Biol. *141*, 1625–1636.

Hobert, O., Schilling, J.W,. Beckerle, M.C., Ullrich, A., Jallal, B. (1996). SH3 domain-dependent interaction of the proto-oncogene product Vav with the focal contact protein zyxin. Oncogene *12*, 1577–1581.

Holt, M.R., and Koffer, A. (2001). Cell motility. proline-rich proteins promote protrusions. Trends Cell Biol. *11*, 38–46.

Horwitz, A.R., and Parsons, J.T. (1999). Cell migration—movin'on. Science *286*, 1102–1103.

Ishizaki, T., Naito, M., Fujisawa, K., Maekawa, M., Watanabe, N., Saito, Y., and Narumiya, S. (1997). p160ROCK, a Rho-associated coiled-coil forming protein kinase, works downstream of Rho and induces focal adhesions. FEBS Lett. *404*, 118–124.

Jay, D.G. (2000). The clutch hypothesis revisited. ascribing the roles of actin-associated proteins in filopodial protrusion in the nerve growth cone. J. Neurobiol. *44*, 114–125.

Kaverina, I., Krylyshkina, O., Gimona, M., Beningo, K., Wang, Y.L., and Small, J.V. (2000). Enforced polarization, and locomotion of fibroblasts lacking microtubules. Curr. Biol. *10*, 739–742.

Kaverina, I., Krylyshkina, O., and Small, J.V. (1999). Microtubule targeting of substrate contacts promotes their relaxation and dissociation. J. Cell Biol. *146*, 1033–1043.

Krause, M., Sechi, A.S., Konradt, M., Monner, D., Gertler, F.B., and Wehland, J. (2000). Fyn-binding protein (Fyb)/SLP-76-associated protein (SLAP), Ena/vasodilator-stimulated phosphoprotein (VASP) proteins, and the Arp2/3 complex link T cell receptor (TCR)-signaling to the actin cytoskeleton. J. Cell Biol. *149*, 181–194.

Ludin, B., and Matus, A. (1998). GFP illuminates the cytoskeleton. Trends Cell Biol. *8*, 72–77.

Macalma, T., Otte, J., Hensler, M.E., Bockholt, S.M., Louis, H.A., Kalff-Suske, M., Grzeschik, K.H., von der Ahe, D., and Beckerle, M.C. (1996). Molecular characterization of human zyxin. J. Biol. Chem. *271*, 31470–31478.

Machesky, L.M. (1997). Complex dynamics at the leading edge. Curr. Biol. *7*, R164–R167.

Meigs, J.B., and Wang, Y.-L. (1986). Reorganization of alpha-actinin and vinculin induced by a phorbol ester in living cells. J. Cell Biol. *102*, 1430–1438.

Mies, B., Rottner, K., and Small, J.V. (1998). Immunofluorescence microscopy of the cytoskeleton: double and triple immunofluorescence II. In: Cell Biology: A Laboratory Handbook, 2nd ed., ed. J.E. Celis, San Diego, CA: Academic Press, 469–472.

Nakagawa, H., Miki, H., Ito, M., Ohashi, K., Takenawa, T., and Miyamoto, S. (2001). N-WASP, WAVE, and Mena play different roles in the organization of actin cytoskeleton in lamellipodia. J. Cell Sci. *114*, 1555–1565.

Niebuhr, K., Ebel, F., Frank, R., Reinhard, M., Domann, E., Carl, U.D., Walter, U., Gertler, F.B., Wehland, J., and Chakraborty, T. (1997). A novel proline-rich motif present in ActA of *Listeria monocytogenes* and cytoskeletal proteins is the ligand for the EVH1 domain, a protein module present in the Ena/VASP family. EMBO J. *16*, 5433–5444.

Niebuhr, K., Lingnau, A., Frank, R., and Wehland, J. (1998). Rapid procedures for preparing monoclonal antibodies and identifying their epitopes. In: Cell Biology: A Laboratory Handbook, 2nd ed., vol. 2, San Diego, CA: Academic Press, 398–403.

Nix, D.A., and Beckerle, M.C. (1997). Nuclear-cytoplasmic shuttling of the focal contact protein, zyxin: a potential mechanism for communication between sites of cell adhesion and the nucleus. J. Cell Biol. *138*, 1139–1147.

Parast, M.M., and Otey, C.A. (2000). Characterization of palladin, a novel protein localized to stress fibers, and cell adhesions. J. Cell Biol. *150*, 643–656.

Reinhard, M., Jouvenal, K., Tripier, D., and Walter, U. (1995). Identification, purification and characterization of a zyxin-related protein that binds the focal adhesion and microfilament protein VASP (vasodilator-stimulated phosphoprotein). Proc. Natl. Acad. Sci. USA *92*, 7956–7960.

Reinhard, M., Rüdiger, M., Jockusch, B.M., and Walter, U. (1996). VASP interaction with vinculin: a recurring theme of interactions with proline-rich motifs. FEBS Lett. *399*, 103–107.

Reinhard, M., Zumbrunn, J., Jaquemar. D., Kuhn, M., Walter, U., and Trueb, B. (1999). An alpha-actinin binding site of zyxin is essential for subcellular zyxin localization and alpha-actinin recruitment. J. Biol. Chem. *274*, 13410–13418.

Ridley, A.J., and Hall, A. (1992). The small GTP-binding protein rho regulates the assembly of focal adhesions and action stress fibers in response to growth factors. Cell *70*, 385–395.

Rottner, K., Hall, A., and Small, J.V. (1999a). Interplay between Rac and Rho in the control of substrate contact dynamics. Curr. Biol. *9*, 640–648.

Rottner, K., Behrendt, B., Small, J.V., and Wehland, J. (1999b). VASP dynamics during lamellipodia protrusion. Nat. Cell Biol. *1*, 321–322.

Salgia, R., Li, J.-L., Lo, S.H., Brunkhorst, B., Kansas, G.S., Sobhany, E.S., Sun, Y., Pisick, E., Hallek, M., Ernst, T., Tantravahi, R., Chen, L.B., and Griffin, J.D. (1995). Molecular cloning of human paxillin, a focal adhesion protein phosphorylated by p210BCR/Abl. J. Biol. Chem. *270*, 5039–5047.

Small, J.V., Rottner, K., Kaverina, I., and Anderson, K.I. (1998). Assembling an actin cytoskeleton for cell attachment and movement. Biochim. Biophys. Acta *1404*, 271–281.

Schulze, H., Huckriede, A., Noegel, A.A., Schleicher, M., and Jockusch, B.M. (1989). Alpha-actinin synthesis can be modulated by antisense probes and is autoregulated in non-muscle cells. EMBO J. *8*, 3587–3593.

Sechi, A.S., Wehland, J., and Small, J.V. (1997). The isolated comet tail pseudopodium of *Listeria monocytogenes*: a tail of two actin filament populations. Long and axial and short and random. J. Cell Biol. *137*, 155–167.

Temm-Grove, C.J., Jockusch, B.M., Rohde, M., Niebuhr, K., Chakraborty, T., and Wehland, J. (1994). Exploitation of microfilament proteins by *Listeria monocytogenes*: microvillus-like composition of the comet tails and vectorial spreading in polarized epithelial sheets. J. Cell Sci. *107*, 1951–1960.

Uehata, M., Ishizaki, T., Satoh, H., Ono, T., Kawahara, T., Morishita, T., Tamakawa, H., Yamagami, K., Inui, J., Maekawa, M., and Narumiya, S. (1997). Calcium sensitization of smooth muscle mediated by a Rho-associated protein kinase in hypertension. Nature *389*, 990–994.